10th ANKARA INTERNATIONAL AEROSPACE CONFERENCE **AIAC-2019-121**
18-20 September 2019 - METU, Ankara TURKEY

AERODYNAMIC DESIGN AND ANALYSIS OF A 7M*5M CLOSED CIRCUIT SUBSONIC WIND TUNNEL

Emre Yüca[1], Mehmet Şerif Kavsaoğlu[2] and Gökhan Durmuş[3]
Eskişehir Teknik Üniversitesi
Eskişehir, Türkiye

ABSTRACT

Aerodynamic design of a closed-circuit subsonic wind tunnel, with 7mx5m test section, is performed. The test section length is 18m. The design flow velocity in the test section is considered to be 100 m/s. The test section enlarges slightly in the flow direction to compensate boundary layer growth. An 8:1 contraction ratio is selected to obtain, as much as possible, uniform and low turbulence flow in the test section. The contraction cone angle is 30° and side surface geometries are obtained by using two third order polynomials. The diffuser sections of the tunnel have not more than 2.5° expansion angles to prevent flow separations. All the rectangular cross sections of the tunnel are cut by isosceles right triangles to obtain octagonal cross sections to eliminate losses and non-uniformities related to corners. An empirical study is performed to estimate losses in different components of the wind tunnel circuit. CFD studies are performed to visualize flow quality, determine the improvement areas and estimate losses.

INTRODUCTION

Wind tunnels are used to determine the forces and moments acting on the objects that are moving through the air or air flow happening around them. The flow field around these objects can also be examined by wind tunnel experiments. There are various sources which explain the fundamentals of wind tunnel design [Pankhurst and Holder,1952; Gorlin and Slezinger, 1966; Barlow et al., 1999]. German Dutch Wind Tunnels [DNW, 2019], Large Low Speed Facility (LLF) is one of the best-known examples to low speed industrial wind tunnels of large test section [Jaarsma and Seidel, 1978]. Ankara Wind Tunnel (ART) was constructed in the late 1940s. It remained un-operational for some years. After the modernization works of 1990s the tunnel entered into service again. With 3.05m*2.44m test chamber cross section, 750 KW motor power and around 80 m/s test section airspeed it is still the leading low speed wind tunnel in Turkey [Mühendis ve Makina, 2011; SAGE, 2019].

In this study, a wind tunnel with 7m * 5m test chamber cross - sectional area was designed and analyzed. The tunnel loop consists of 4 arms. At the junction of both arms is located a corner. The elements in the first arm are settling chamber, collector, test chamber and first diffuser. In the second arm the second diffuser is located, the third arm includes the propeller block and the third (main) diffuser, and the fourth arm includes the fourth diffuser. The total

[1] Reserch Assistant in Dept. of Airframe and Powerplant Maintenance, Email: emreyuca@ eskisehir.edu.tr
[2] Prof., Dept. of Airframe and Powerplant Maintenance, Email: mskavsaoglu@eskisehir.edu.tr
[3] Dr. Faculty Member, Dept. of Airframe and Powerplant Maintenance, Email: gdurmus@eskisehir.edu.tr

expansion rate of the diffusers should be approximately equal to the contraction ratio of the collector. The reason for this approximate equality is that the test chamber is slightly widened to compensate for the boundary layer thickening.

WIND TUNNEL DESIGN

Test Chamber Inlet Cross Section:

Initially, the cross section of the test chamber was considered as rectangular with 7m * 5m dimension. However, in many wind tunnels, octagonal cross-section instead of rectangular section is preferred. The CFD solutions made during studies for the collector design have shown that the flow creates a static pressure distribution in accordance with the circular cross-section. Corner currents in a rectangular geometry can adversely affect the flow quality. It can be said that the flow around the corners in a rectangular geometry does not contribute significantly to the effective test area. By clipping these corners, for the same mass flow rate, faster and better-quality flow can be obtained in the central regions of the tunnel.

Octagonal geometry was formed by clipping at a 45° angle, up to a quarter of a short edge (1.25 m) from each edge. Comparison of rectangular and octagonal geometries is given in Table 1. According to this table, the cross-sectional area decreases 8.93% by trimming the corners. This means that less power will be spent for the same speed. Also, the area around the test chamber decrease by 12.20 %. This means that at the same speed, the tunnel walls will create less skin friction. On the other hand, hydraulic diameter increases by 3.74 % which may be considered as positive. Inlet cross section of test chamber is shown in Figure 1.

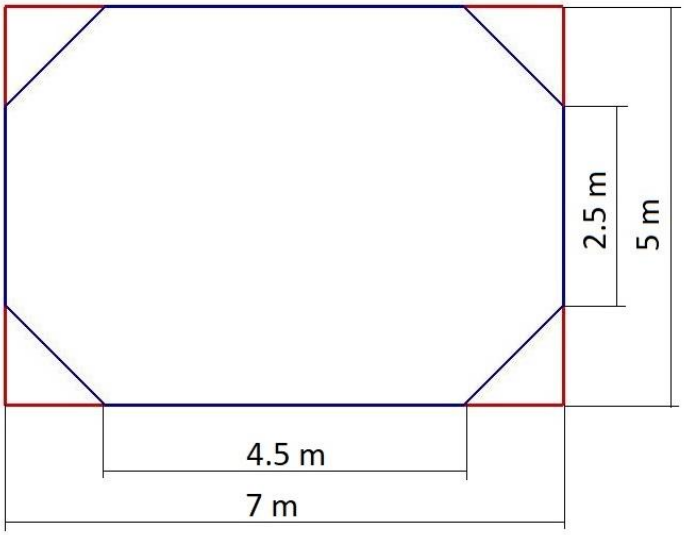

Figure 1. Inlet cross section of octagonal test chamber

Table 1. Comparison of rectangular and octagonal geometries.

	Rectangular	**Corners clipped with 45°**	**% difference**
Area, A	7×5=35 m^2	7×5-4×0.5×1.25×1.25 = 31.875 m^2	-8.93
Perimeter, P	7+5+7+5=24m	(4.5+2.5)*2+1.7678*4 = 21.0712	-12.20
Hydraulic Diameter, d_h=(4A)/P	5.833 m	6.0509 m	+3.74

Test Chamber Length

For aeronautical applications, it is advised that the Test Chamber length should be around one to two times the length of the Test Chamber main edge [Barlow et al., 1999]. For the designed wind tunnel, long edge of the Test Chamber inlet is 7m. Then, Test Chamber length should be around 7-14 m. On the other hand, the flow at the contraction exit is not sufficiently uniform and a constant area section is needed, after the contraction, to improve the flow uniformity [Barlow et al, 1999]. We may consider the length of this part as 2m. Then, the Test Chamber length should be around 9-16 m. In Table 2, Test Chamber length to hydraulic diameter ratios of some existing tunnels are presented [DNW, 2019; SAGE, 2019; RUAG, 2019; NRC, 2019].

Table 2. Test Chamber Length to Hydraulic Diameter Ratios of some wind tunnels.
(*): Corner trims are taken into account

Tunnel	Hydraulic Diameter, d_h	Test Chamber Length, L	L/d_h
DNW-LLF 6m*6m	6 m	15 m	2.50
DNW-LLF 8m*6m	6.86 m	20 m	2.92
DNW-LLF 9.5m*9.5m	9.5 m	20 m	2.11
ART 3.05m*2.44m, trimmed corners	2.81 m (*)	6.10 m	2.17 (*)
RUAG 7m*5m, trimmed corners	6.05 m (*)	15 m	2.48 (*)
NRC 9.1m*9.1m	9.1 m	24 m	2.64

In the tunnel, experiments can also be carried out for automotive, construction and city planning. Taking these into account, it is useful not to make the experiment room too short. However, if it is too long then the frictional losses increase. Pankhurst and Holder stated that if the test chamber is kept long, the power demand will increase slightly, and recommended that the test chamber length be at least 3 times the diameter. [Pankhurst and Holder, 1952]. Finally, 18 meter is decided as the test chamber length. Test chamber length to hydraulic diameter ratio is given in Table 3.

Table 3. Designed 7m*5m Wind Tunnel Test Chamber Length to Hydraulic Diameter Ratio.

Tunnel	Hydraulic Diameter, d_h	Test Chamber Length, L	L/d_h
7m*5m (corners trimmed 45°)	6.05 m	**18 m**	**2.98**

Test Chamber Outlet Cross Section

The test chamber outlet section should be larger than the inlet section due to the thickening of the boundary layer throughout the test chamber. The area of the test chamber outlet section is calculated by shifting the walls of the outlet section outward by the boundary layer displacement thickness. Boundary Layer Displacement Thickness, δ^*, is defined as:

$$\delta^* = \int \left(1 - \frac{u}{U_e}\right) dy$$

Here, $u = u(y)$, is the velocity distribution inside the boundary layer. U_e, is the velocity at the edge of the boundary layer. y, is the distance perpendicular to wall. With a rough approach, it is recommended that the walls of the test chamber be opened out at a half degree angle [Barlow et al., 1999]. Then for 18-meter test chamber length:

$$\tan(0.5) = \frac{dr}{L}$$

$$dr = 18 * \tan(0.5) = 0.1571m = 15.71\ cm$$

That is, the outlet cross-sectional area will be obtained by translating each wall 15.71 cm outward when compared to the inlet cross-section.

An empirical formula for the calculation of displacement thickness is as follows [Schetz, 1993].

$$\frac{\delta}{x} = \frac{0.375}{Re_x^{1/5}}$$

$$\frac{\delta^*}{\delta} = \frac{1}{8}$$

First, we need to calculate the Reynolds number.

$$Re_x = \frac{\rho U_e x}{\mu}$$

Assuming the wind tunnel is located at an altitude of 900 meter above sea level at standard atmosphere conditions and 100 m/s test chamber speed;
$\rho = 1.123\ kg/m^3$ (density)
$\mu = 1.783 * 10^{-5}\ \frac{Ns}{m^2}$ veya $\frac{kg}{ms}$ (viscosity)

$$Re_x = \frac{1.123 \times 100 \times 18}{1.783 \times 10^{-5}} = 1.134 \times 10^8$$

For test chamber divergence angle calculation using an average Reynolds number may be more suitable. The Reynolds Number at the mid-section of the test chamber (x=9 m) is $Re_x = 5.67 \times 10^7$.

Results are summarized in Table 4.

Table 4. For 100 m/s airspeed and 900 m altitude test chamber displacement thickness calculation results.

x	Re_x	δ	δ^*	$\frac{\delta^*}{x} = \frac{dr}{L}$	$\gamma = \text{atan}\left(\frac{dr}{L}\right)$
9 m	5.67×10^7	0.095 m (9.50 cm)	0.0119 m (1.19 cm)	0.0013	0.076°
18 m	1.134×10^8	0.1653 m (16.53 cm)	0.0207 m (2.07 cm)	0.0012	0.069°

If we consider test chamber walls divergence angle as $\gamma = 0.077°$;

$$dr = Ltan(\gamma) = 18 * \tan(0.077) = 0.0242m\ (2.42cm)$$

Which means hydraulic radius is 2.42 cm longer at the outlet when compared to inlet.
Inlet section hydraulic diameter: $d_{h,inlet} = 6.05\ m$
Outlet section hydraulic diameter: $d_{h,outlet} = 6.05 + 2 * 0.0242 = 6.0984\ m\ \cong 6.1\ m$

$$\frac{A_{outlet}}{A_{inlet}} = \frac{d_{h,outlet}^2}{d_{h,inlet}^2} = \frac{6.10^2}{6.05^2} = 1.017$$

Outlet area is about 1.7 % more than the inlet area. This can be achieved by reducing the 45° corner fillet sizes at the outlet. At other cross sections fillet size decreases linearly from inlet to outlet. Thus, test chamber top wall can be made parallel to bottom wall and side walls can be made parallel to each other. A higher divergence angle then this calculated value ($\gamma = 0.077°$) may be needed due to blockage caused by model, support etc. Exit cross section of the test

chamber is shown in Figure 2, and three-dimensional view of the test section is shown in Figure 3.

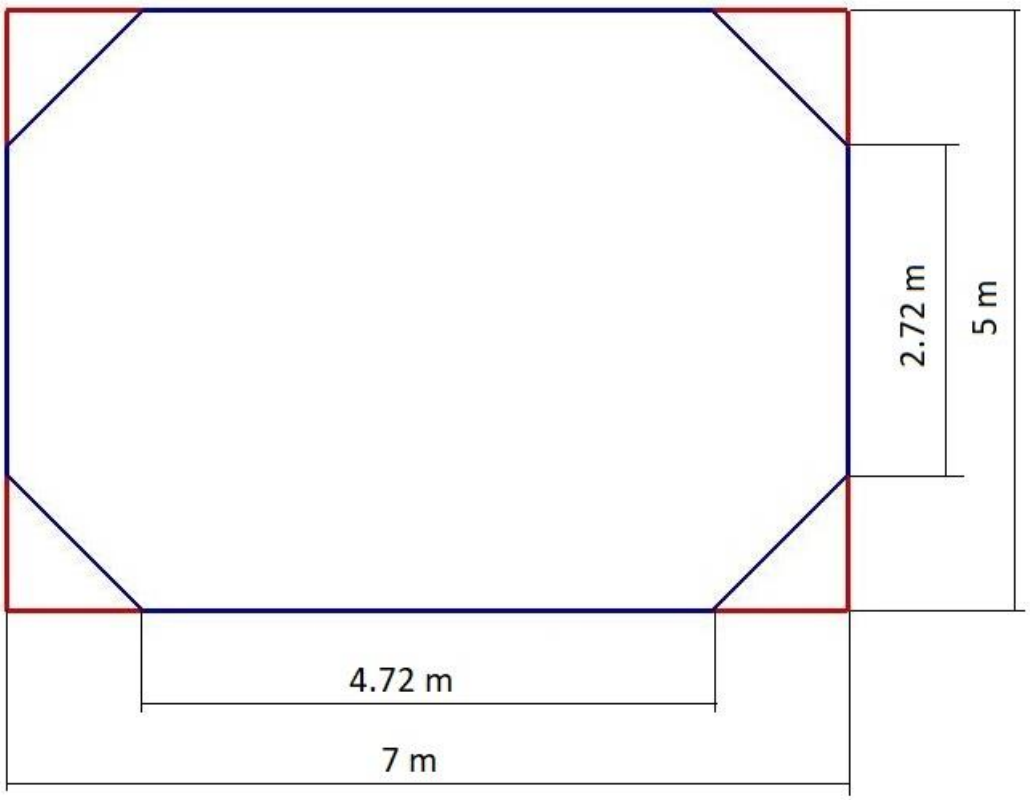

Figure 2. Outlet cross section of the test chamber.

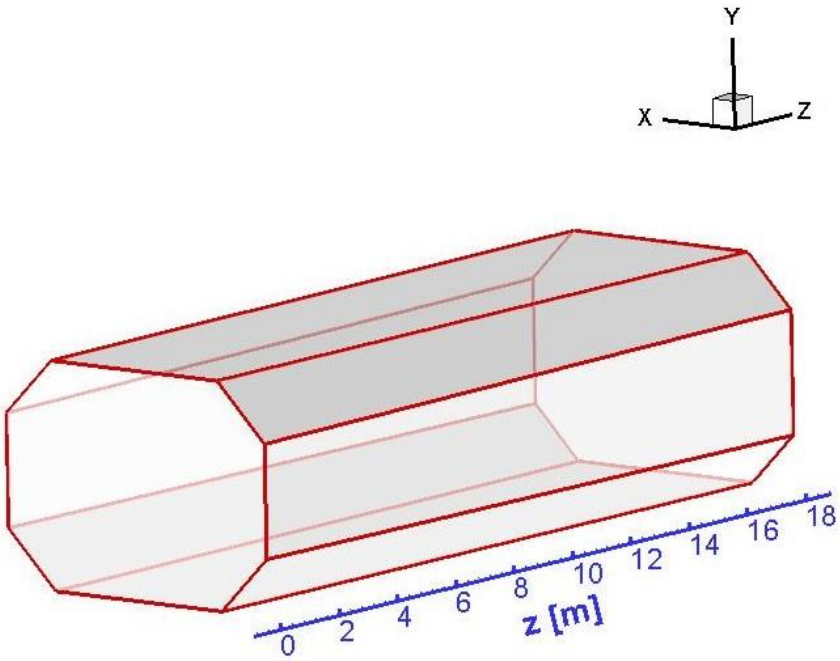

Figure 3. Three-dimensional view of the test chamber.

Contraction:

The contraction geometry is described in Figure 2. Here, the index 1 represents the output section and the index 2 represents the input section. The inflection point is the point where the slope of the curve passes from the increment to the decrease. “r” is the hydraulic radius, “α” is the collector peak angle, “θ_i” is the angle made by the x-axis of the line which is tangent to the curve at the inflection point. L represents the contraction length, and L_i represents the position of the inflection point. Selection of small contraction half-apex angle (α / 2) positively affects the quality of the outflow [Gorlin and Slezinger, 1966]. On the other hand, if this angle is too small, losses will increase due to longer contraction length. The angle of the tangent line at the inflection point (θ_i) is selected slightly above the contraction half-apex angle.

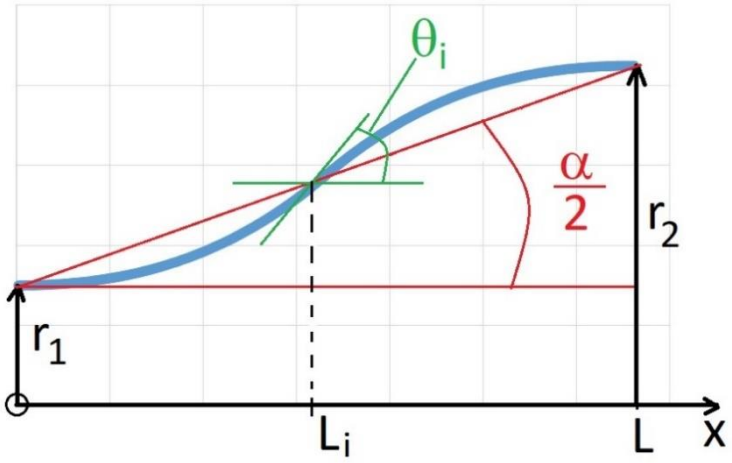

Figure 4. Contraction geometry

Selection of the Area Ratio:

$$\frac{A_2}{A_1} = 8.0$$

Apex Angle:

$$\alpha = 30°$$

$$\frac{\alpha}{2} = 15°$$

$$\tan\left(\frac{\alpha}{2}\right) = 0.2679$$

Outlet section long edge = 7m
Outlet section short edge = 5m
Outlet cross section area = 7m*5m = 35 m^2
Outlet section hydraulic diameter:

$$d_{h1} = \frac{4A_1}{P_1} = \frac{4 * 35}{2 * (7 + 5)} = 5.833m$$

Outlet section hydraulic radius:

$$r_{h1} = 2.9165\ m$$

Inlet section long edge = $7 * \sqrt{8} = 19.7990\ m$
Inlet section short edge = $5 * \sqrt{8} = 14.1421\ m$
Inlet cross section area = $A_1 = 19.7990 * 2.8284 = 280$ m^2
Inlet section hydraulic diameter:

$$d_{h2} = \frac{4A_2}{P_2} = \frac{4 * 280}{2 * (19.7990 + 14.1421)} = 16.4992m$$

Inlet section hydraulic radius:

$$r_{h2} = 8.4853\ m$$

Contraction Length:

$$tan\left(\frac{\alpha}{2}\right) = \tan(15) = 0.2679 = \frac{r_{h2} - r_{h1}}{L} = \frac{8.4853 - 2.9165}{L}$$

$$L = 19.9071\ m$$

Design of the Contraction Side Surfaces

Based on hydraulic diameter a curve is determined to represent contraction side surface. This curve is made of two third order polynomials. The selected coordinate system and polynomials are described in Figure 5. In this figure, r_1 and r_2 represent the contraction outlet and inlet hydraulic radiuses respectively. The first polynomial represents the geometry between outlet ($x = 0$) and the inflection point ($x = L_i$) where the slope of the curve changes from ascending to descending character. The second polynomial defines the region between the inflection point and the inlet ($x = L_i$). This way of defining the contraction curve was also utilized by other designers such as [Hernandez et al., 2013] and [Kao et al., 2017]. If the length of the contraction, inlet and outlet radiuses and inlet and outlet slopes are fixed values then, x coordinate of the inflection point (L_i), r coordinate of the inflection point (r_i), and the slope of the inflection point (m_i) emerge as free variables. This gives us the opportunity to obtain many curves for the same inlet to outlet area ratio and same contraction length.

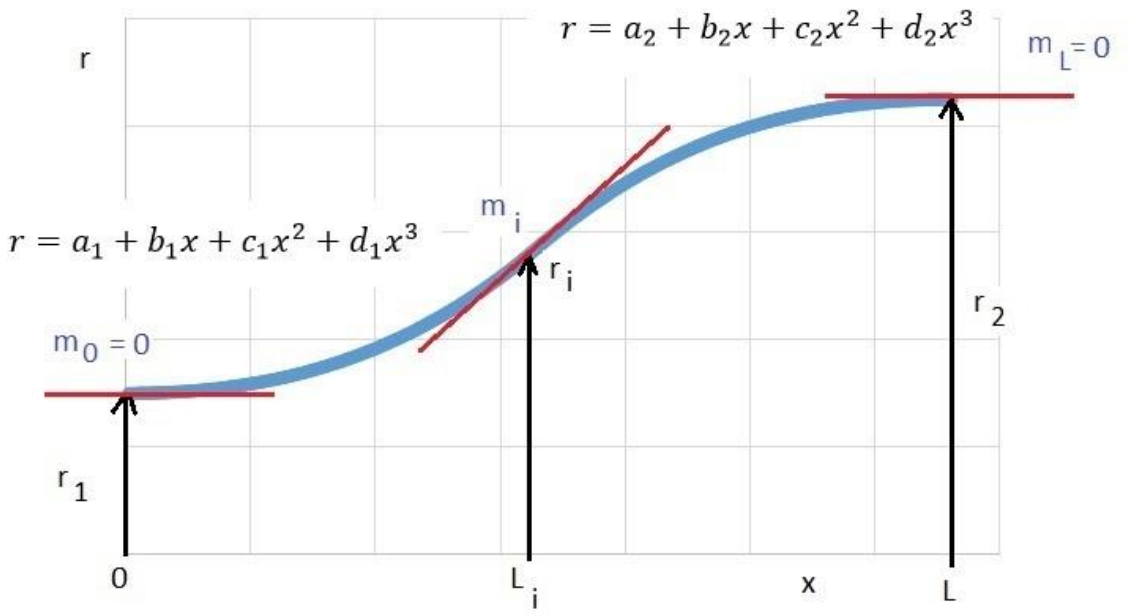

Figure 5. Polynomials which represent the contraction curve.

Design parameters of the contraction curve are selected as:
Distance from outlet to inflection point: $L_i = 0.5L$
Hydraulic Radius of the inflection point: $r_i = \frac{r_1+r_2}{2.4}$
Tangent angle at the inflection point: $\theta_i = 25°$

Designed contraction curve is presented in Figure 6.

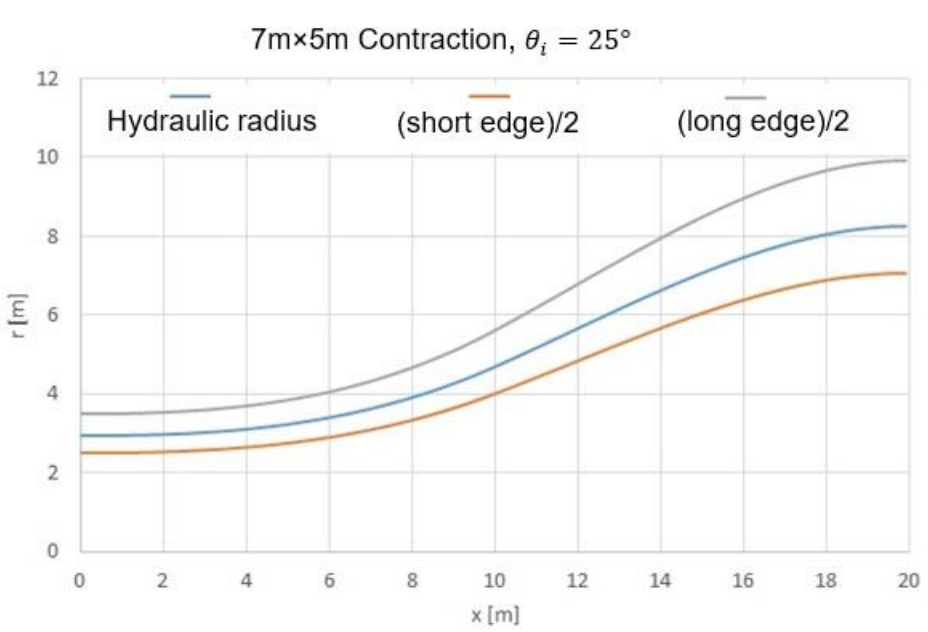

Figure 6. Contraction curve

Similar to the test section, contraction corners are also trimmed to obtain octagonal cross sections. At a given cross section, isosceles right triangles are cut from each corner of the initial rectangular cross section. Each short edge of these triangles is equal to the ¼ of the short edge of the rectangle at that section. Final, three-dimensional view of the contraction geometry is shown in Figure 7.

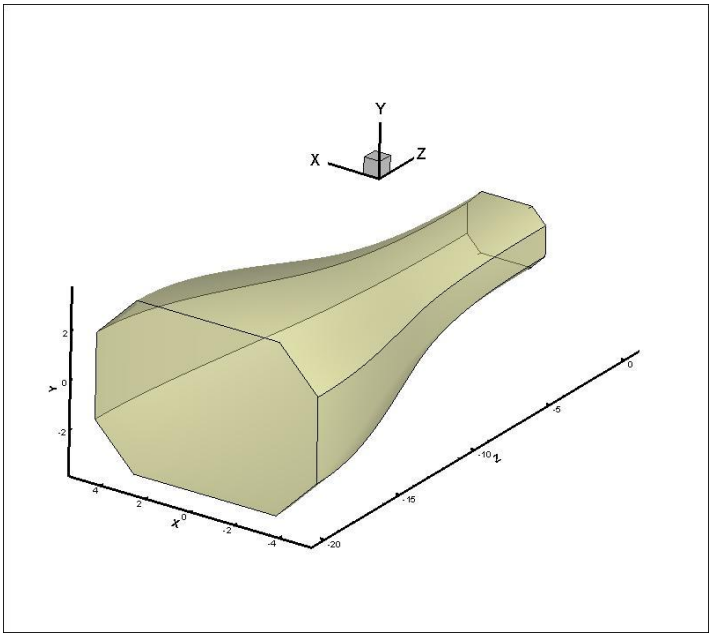

Figure 7. The three-dimensional view of the contraction geometry

Settling Chamber

Settling chamber is the constant area section before the contraction entrance. Honeycomb and screens are located in this section. Settling chamber length is taken as half of the contraction length.

$$L_{set.c.} = \frac{L_{contraction}}{2} = \frac{19.9027}{2} = 9.9514\ m$$

Design of Diffusers

In this wind tunnel:
Contraction inlet area = 255 m^2
Test Chamber outlet area = 32.417 m^2
Total diffuser expansion ratio $= \frac{255}{32.417} = 7.87$
This area ratio is provided by four diffusers.

[Barlow et al., 1999] advises that equivalent cone angle of a diffuser should be around 2°-3.5° and diffuser outlet to inlet area ratio should be around 2-3. The area ratio of the first diffuser is selected as 2.0 and the expansion angle is 2.5°. For other diffusers, the expansion angle is chosen not more than 2.5°. First diffuser's inlet section is same as the test chamber outlet section. Hydraulic diameter of the first diffuser inlet is calculated as follows:

Inlet Area: $A_{1.dif.in.} = 7 * 5 - 4 * (0.5 * 1.14 * 1.14) = 32.4008$
Inlet Perimeter: $P_{1.dif.in.} = 4.72 * 2 + 2.72 * 2 + 4 * (1.14^2 + 1.14^2)^{0.5} = 21.3288$
Hydraulic Diameter: $D_{h,1.dif.in.} = 4 * \frac{A}{P} = 6.076437\ m$
Hydraulic Radius: $r_{h,1.dif.in.} = 3.038219\ m$

First diffuser outlet area:

$$A_{1.dif.out.} = 2 \times A_{1.dif.in.} = 2 \times 32.4008 = 64.8016\ m^2$$

Outlet cross section of the first diffuser is an equilateral octagonal. Each edge of this octagonal is calculated as:

$A_{1.dif.çık.} = 64.8016\ m^2 = \left(\frac{1}{4}\right) * n * a^2 * \cot\left(\frac{\pi}{n}\right) = \left(\frac{1}{4}\right) * 8 * a^2 * \cot(\pi/8)$
(n: number of edges,a: edge length)

$$a = 3.6634\ m$$

Hydraulic diameter of the first diffuser outlet is found as,
Outlet perimeter: $P_{1.dif.out.} = 3.6634 * 8 = 29.3072$ m
Outlet hydraulic diameter: $D_{h,1.dif.out.} = 4 * \frac{A}{P} = 8.84424\ m$
Outlet hydraulic radius: $r_{h,1.dif.out.} = 4.42212\ m$

For 2.5° expansion angle, first diffuser's length is calculated as;

$$L_{1.dif.} = \frac{(r_{h,1.dif.out.} - r_{h,1.dif.in.})}{\tan(2.5°)} = \frac{4.4221 - 3.0382}{\tan(2.5°)} = 31.6965\ m$$

Three-dimensional view of the first diffuser is shown in Figure 8.

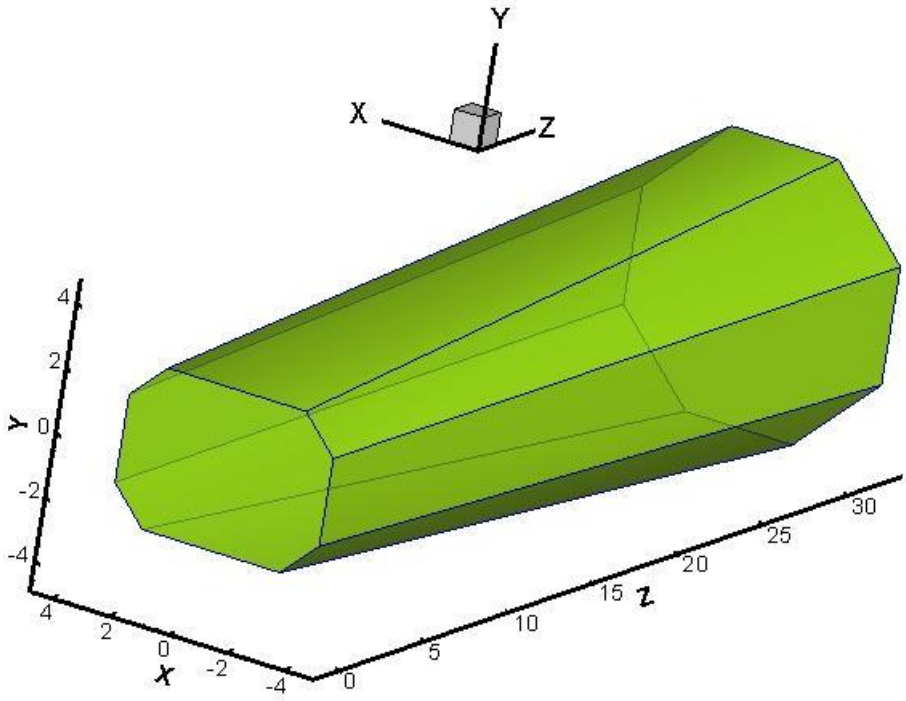

Figure 8. Three-dimensional view of the first diffuser.

Before designing the other three diffusers we may approximately estimate the total length of the diffusers from Figure 9. First diffuser inlet area is equal to the test chamber outlet area and fourth diffuser exit area is equal to the settling chamber inlet area. Total length of the diffusers can be estimated to satisfy 2.5° expansion angle criteria.

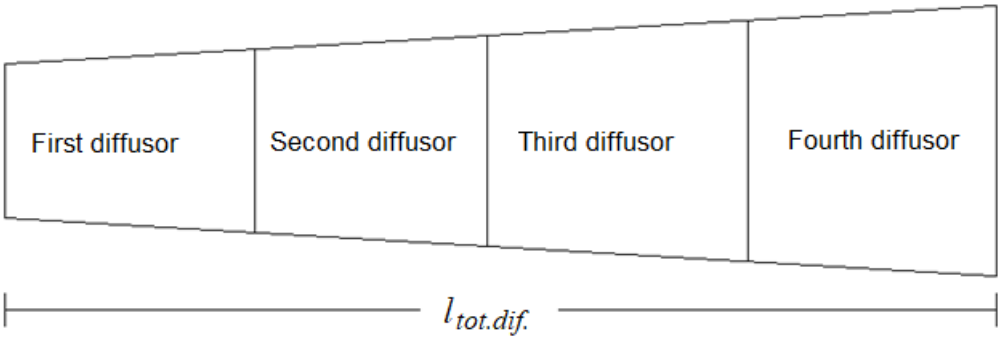

Figure 9. Total Length of the Diffusers.

$$\tan(2.5°) = \frac{r_{h,4.dif.out.} - r_{h,1.dif.in.}}{l_{tot.dif.approx.}}$$

$$0.0436609 = \frac{8.557335 - 3.038219}{l_{tot.dif.approx.}}$$

$$l_{tot.dif.approx.} = 126.408539\ m$$

If we ignore the differences of the hydraulic diameters of the second and forth diffusers we may roughly estimate the total length of the third diffuser and the fan section as equal to the total length of the settling chamber, contraction, test chamber and the first diffuser.

Settling chamber length, $l_{set.\ c.} = 9.95135\ m$
Contraction length, $l_{contraction} = 19.9027\ m$
Test chamber length, $l_{test\ chamber} = 18\ m$
First diffuser length, $l_{1.dif.} = 31.6978123\ m$

$$l_{set.c.} + l_{contraction} + l_{test\ chamber} + l_{1.dif.} = 9.95135 + 19.9027 + 18 + 31.6978123$$
$$= 79.5518623\ m$$
$$l_{3.dif.approx.} + l_{fan\ approx.} = 79.5518623\ m$$

In this equation;
$l_{3.dif.approx.}$: Approximate length of the third diffuser
$l_{fan\ approx.}$: Approximate length of the fan section

For, DLR-LLF wind tunnel, fan section length to third diffuser length ratio is [Jaarsma and Seidel, 1978];

$$\frac{l_{fan}}{l_{3.dif.}} = 0.50209$$

If we use the same ratio;

$$l_{3.dif.approx.} + l_{fan\ approx.} = l_{3.dif.} + 0.50209 \times l_{3.dif.} = 79.5518623\ m$$
$$l_{3.dif.approx.} = 52.960782\ m$$
$$l_{fan\ approx.} = 26.5911\ m$$

Finally after some analysis, the main dimensions of the wind tunnel are shown in Figure 10.

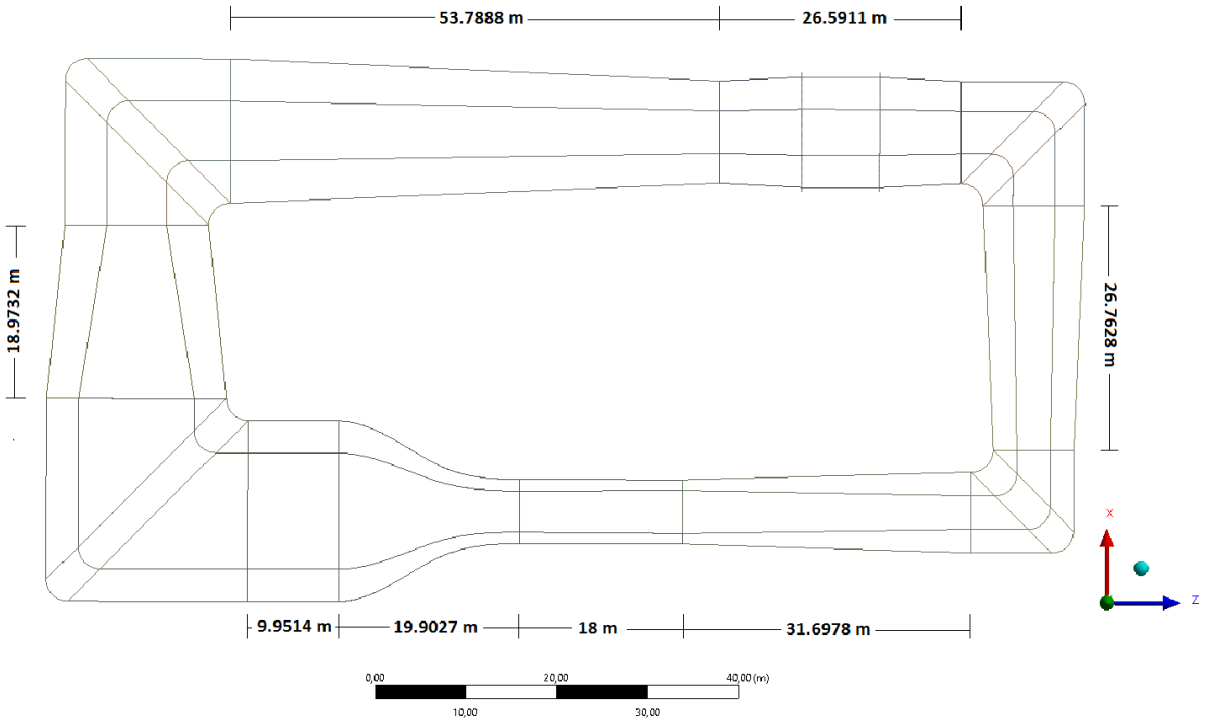

Figure 10. Main dimensions of the wind tunnel.

Design of Fan Block

The fan block is divided into three parts as “fan input zone”, “fan zone” “and “fan output zone” as in Figure 11.

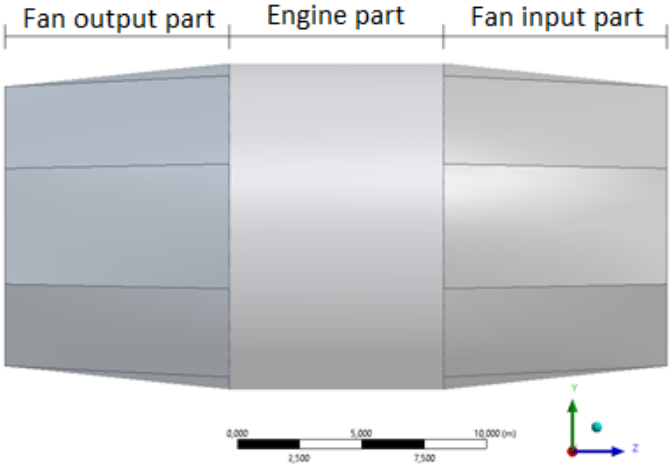

Figure 11. Top view of propeller block

Fan input section length:9 m
Fan output section length:9 m
Propeller section length:8.5911 m
Propeller section diameter: $D = 13.0656\,m$

Corner Design:

The input and output section of each corner of the wind tunnel is the same as the outlet section of the diffuser before it. At all corners, the turning radius is taken r = 2.4 m. Top view and the dimensions of the inlet-outlet section of the first corner are given in Figure 12.

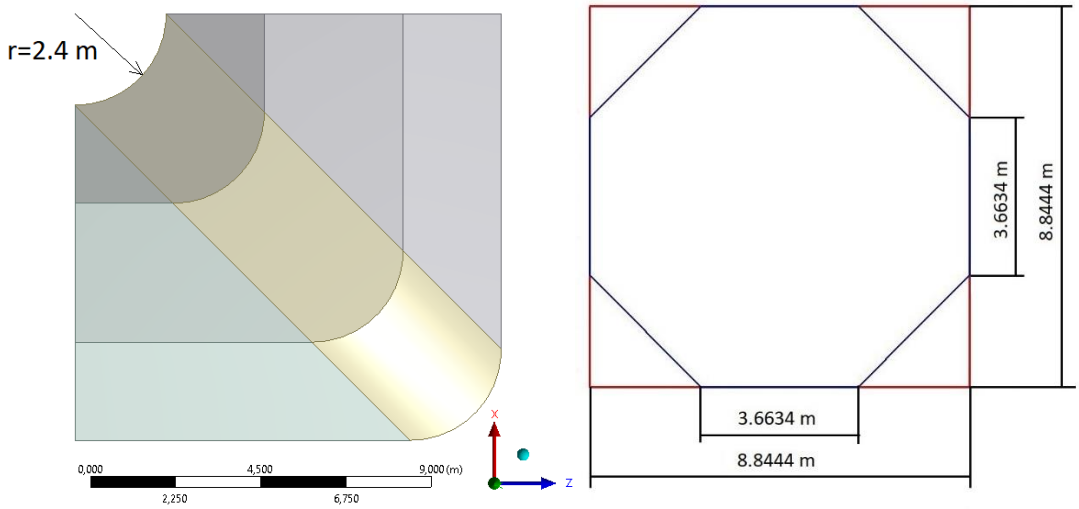

Figure 12. Top view and the dimensions of the inlet-outlet section of the first corner

Three-dimensional view of the wind tunnel with all components is given in Figure 13.

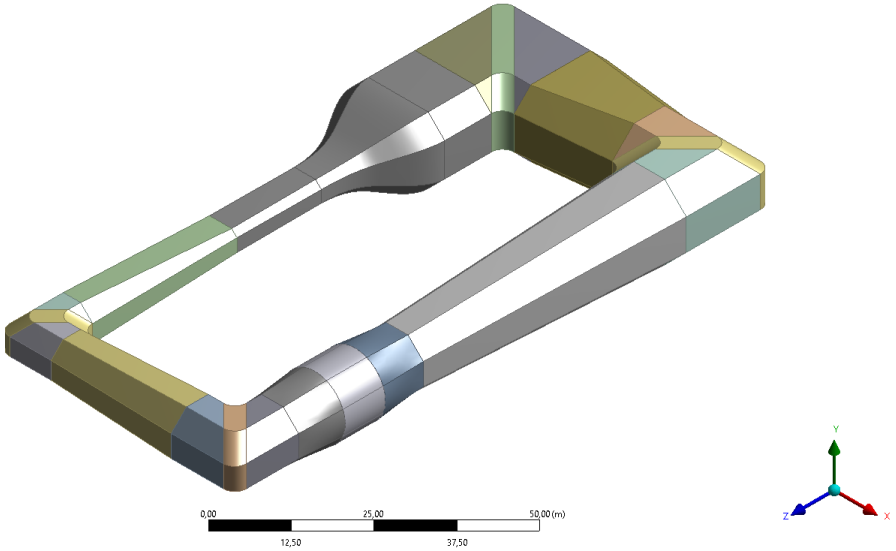

Figure 13. Three-dimensional view of the wind tunnel.

CFD ANALYSIS FOR SETTLING CHAMBER, CONTRACTION AND TEST CHAMBER

CFD analyses are performed by using the Fluent software. As a result of the analysis, the velocity contours obtained in the plane of symmetry and the static pressure contours obtained in the contraction outlet plane are given in Figure 14 and Figure 15.

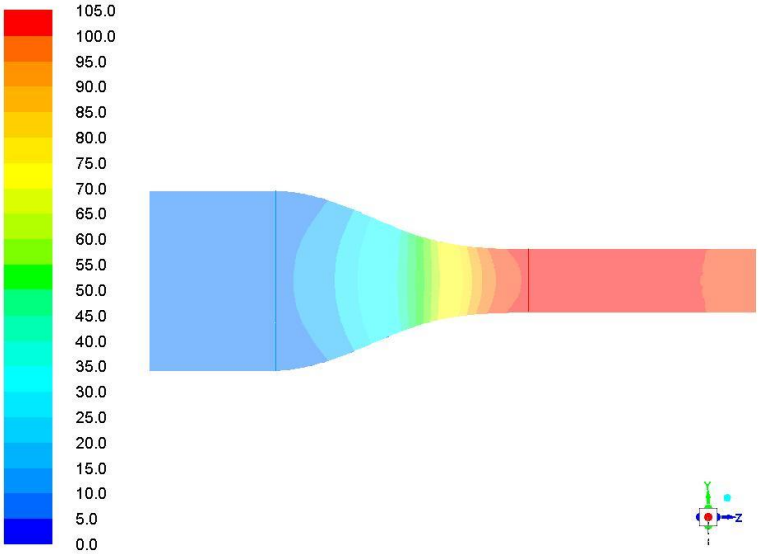

Figure 14: Velocity contours in the symmetry plane (m/s)

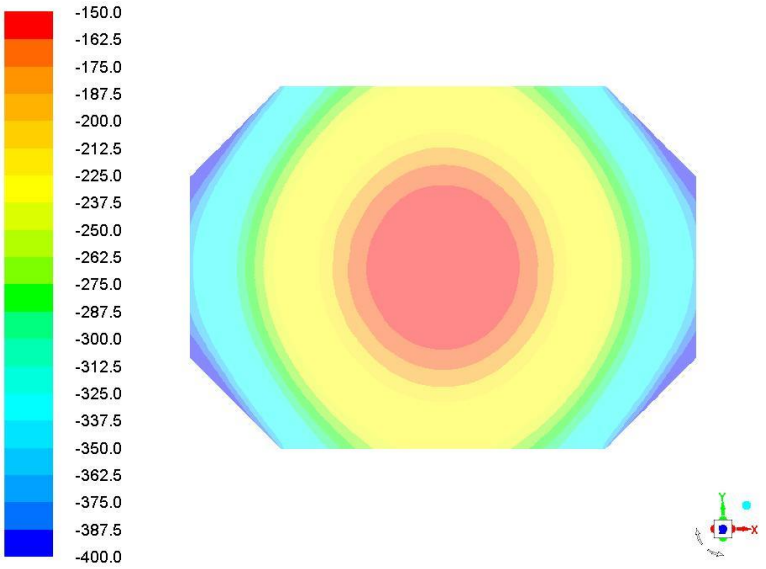

Figure 15. Static pressure contours at the contraction outlet plane (Pascal).

Based on the computational study, flow quality estimates at the different cross sections of the test chamber are summarized in Table 5. We may say that the nonuniformities at the contraction outlet reduces to a reasonable level 2m after the contraction outlet.

Table 5. Flow quality estimates at different cross sections of the test chamber

	Average speed except boundary layer (m/s)	Standard deviation from average speed (m/s)	Maximum deviation from average speed (m/s)	Standard angular deviation of the speed vector (°)	Maximum angular deviation (°)
Contraction outlet	101,5474	0,505462	1,075422	0,070033	0,46464
1 m after the contraction outlet	101,3527	0,172056	0,416743	0,047084	0,20464
2 m after the contraction outlet	101,2043	0,063175	0,15735	0,05943	0,225286
50% of the test chamber	100,4936	0,007765	0,035639	0,061829	0,265316
75% of the test chamber	100,0549	0,008565	0,042946	0,062701	0,259387

ESTIMATION OF ENERGY RATIO

The empirical method for the estimation of wind tunnel components energy losses is explained by [Barlow et al., 1999]. The calculated loss coefficients for all components of the wind tunnel and energy ratio are given in Table 6. The flow rate in the test chamber is 100 m/s. The tunnel temperature is 20 ° C. In the given table, K_l is the coefficient of loss of the related component and K_{lt} is the coefficient in which the local loss coefficient is correlated with the $K_{lt} = K_l * \frac{q_l}{q_t}$ equation with the dynamic pressure of the test chamber. In the equation, q_l is the dynamic pressure in the inlet cross-section of the wind tunnel component and q_t is the dynamic pressure in the test chamber. The Δp values in the table are calculated by the

equation $\Delta p = K_{lt} * q_i = K_{lt} * (1/2 * \rho * V_i{}^2)$. In this equation, the dynamic pressure (q_i) and velocity (V_i) are the values in the input section of the respective component.

Table 6. The calculated loss coefficients for all components of the wind tunnel and energy ratio

Component	**Δp (Pa)**	K_l	K_{lt}	**Total loss (%)**
Test chamber	120.6	0.0199	0.0199	14.76
1. Diffuser	268.98	0.0445	0.0445	33.01
1. Corner	195.78	0.1294	0.0324	24.04
2. Diffuser	43.95	0.0291	0.0073	5.42
2. Corner	78.01	0.1318	0.0129	9.57
3. Diffuser	27.07	0.0457	0.0045	3.34
3. Corner	20.11	0.1357	0.0033	2.45
4. Diffuser	2.02	0.0136	0.0003	0.22
4. Corner	13.38	0.1370	0.0022	1.63
Settling chamber	0.44	0.0045	$7.265*10^{-5}$	0.05
Contraction	44.39	0.4583	0.0074	5.49
Total	**814.73**	**1.1495**	**0.1348**	**100**
$E_R = 1/\sum K_{lt} = 7.42$				

The total test chamber kinetic energy per unit time divided by the energy ratio gives the energy per unit time which needs to be transferred to the wind tunnel air by the fan. For 100 m/s test section velocity and 900 m altitude standard atmosphere:

Test Chamber Mass Flow Rate:

$$\dot{m} = \rho V A = 1.123 \times 100 \times 31.875 = 3577 \ \mathrm{kg/m^3}$$

Test Chamber Kinetic Energy per unit time:

$$\frac{1}{2}\dot{m}V^2 = \frac{1}{2} \times 3577 \times 100^2 = 17{,}885{,}000 \ Watt = 17.885 \ MW$$

Power to be supplied by fan:

$$\frac{17.885}{7.42} = 2.41 \ MW$$

This energy ratio can be considered as optimistic. Losses related to screens, honeycombs, heat exchangers, model and support are not included.

CONCLUSION AND FUTURE WORK

In spite of the advancements in computational aerodynamics wind tunnels are still being used and the need for wind tunnel testing is growing to design competitive aircraft, land vehicles, high speed trains, wind turbines, buildings etc.

In wind tunnel experiments simulation of Mach number, Reynolds number and geometric details is important. Nowadays there are high speed, pressurized and cryogenic wind tunnels. However, these tunnels have relatively small test sections and many times very short test durations. They are quite expensive to built and operate. Low speed tunnels are suitable for many industrial applications. Even for high speed aircraft, many tests are performed at low speed tunnels.

A 7m×5m cross section large low speed wind tunnel conceptual design study is performed. Present research is progressing towards optimized corner wanes etc. In addition to high flow quality, energy efficiency is an important concern. Reducing the losses due to flow separation, surface friction, cooling etc. may be considered as future research areas.

References

Barlow, J.B., Rae, W.H., Pope, A. (1999) *Low Speed Wind Tunnel Testing*, John Wiley and Sons

DNW (2019) https://www.dnw.aero/wind-tunnels/llf/

Gorlin, S. M. And Slezinger I.I. (1966) "Wind Tunnels and Their Instrumentation", Israel Program for Scientific Translations, Jerusalem.

Hernandez, Lopez, Jarzabek, Perales, Wu, Xiaoxiao (2013) "Design Methodology for a Quick and Low-Cost Wind Tunnel" http://cdn.intechopen.com/pdfs/42327/intech-design_methodology_for_a_quick_and_low_cost_wind_tunnel.pdf http://dx.doi.org/10.5772/54169

Jaarsma, F., Seidel, M. (1978) *The German Dutch Wind Tunnel DNW Design Aspects and Status of Construction*, ICAS 1978

Kao, Yi-Huan, Jiang, Zhou-Wei, and Fang, Sheng-Cyuan (2017) "A Computational Simulation Study of Fluid Mechanics of Low-Speed Wind Tunnel Contractions", Fluids 2017, volume 2 issue2, 23; https://doi.org/10.3390/fluids2020023

Mühendis ve Makina (2011) *Ankara Rüzgar Tüneli*, Mühendis ve Makina, Cilt 52, Sayı 614.

http://www.sage.tubitak.gov.tr/tr/hizmetlerimiz/ruzgar-tuneli-test-hizmetleri-0 (Mart 2019 da erişim sağlandı)

NRC (2019) https://nrc.canada.ca/en/research-development/nrc-facilities/9-m-wind-tunnel-research-facility

Pankhurst, R.C., Holder, D. W. (1952) *Wind Tunnel Technique*, Sir Isaac Pitman and Sons

RUAG (2019) https://aerodynamics.ruag.com/en/aerodynamics/aerospace-wind-tunnel

SAGE (2019) http://www.sage.tubitak.gov.tr/tr/hizmetlerimiz/ruzgar-tuneli-test-hizmetleri-0

Schetz J.A. (1993) "Boundary Layer Analysis", Prentice Hall.